

# EEG phase patterns reflect the representation of semantic categories of objects

Mehdi Behroozi<sup>1,2,3</sup> · Mohammad Reza Daliri<sup>1,2</sup> · Babak Shekarchi<sup>4</sup>

Received: 26 July 2014 / Accepted: 7 September 2015  
© International Federation for Medical and Biological Engineering 2015

**Abstract** Oscillations of electroencephalographic signals represent the cognitive processes arose from the behavioral task and sensory representations across the mental state activity. Previous studies have shown the relation between event-related EEG and sensory-cognitive representation and revealed that categorization of presented object can be successfully recognized using recorded EEG signals when subjects view objects. Here, EEG signals in conjunction with a multivariate pattern recognition technique were used for investigating the possibility to identify conceptual representation based on the presentation of 12 semantic categories of objects (5 exemplars per category). Using multivariate stimulus decoding methods, surprisingly, we demonstrate that how objects are discriminated from phase pattern of EEG signals across the time in low-frequency band (1–4 Hz), but not from power of oscillatory brain signals in the same frequency band. In contrast, discrimination accuracy from the power of EEG signals has significantly higher than the performance from phase of EEG

signal in the high-frequency band (20–30 Hz). Moreover, our results indicate that how the accuracy of prediction changes between various areas of brain continuously across the time. In particular, we find that, during the object categorization task, the inter-trial phase coherence in low-frequency band is significantly higher than other frequency in various regions of interests. This measure is associated with decoding pattern across the time. These results suggest that the mechanism underlying conceptual representation can be mediated by the phase of oscillatory neural activity.

**Keywords** Oscillations · Categorization · Delta band · Inter-trial phase coherence · Hilbert transform · Naïve Bayes classifier

## 1 Introduction

The question how mental states are transformed into neural activity patterns is a key challenge in many scientific committees. In the past decade, the two popular neuroimaging methods and noninvasive brain imaging tools have been considered by neuroscientist to find answers to the above question, namely the functional magnetic resonance imaging (fMRI) and electroencephalogram (EEG) [2, 7, 8, 15, 31, 43]. In fMRI, hemodynamic responses reflect the representation pattern of presented object exemplars and they used to predict the object category using fMRI [4, 19, 20]. The previous studies revealed that representation patterns of presented object exemplars are distributed across the cortex and the signals related to a single object from different brain areas have overlaps [6, 17]. These fMRI studies on object categorization tended researcher to use EEG for object categorization due to EEG's good temporal resolutions. The recorded EEG signals from the scalp are

✉ Mohammad Reza Daliri  
daliri@iust.ac.ir

✉ Babak Shekarchi  
shekarchi.babak@yahoo.com

<sup>1</sup> Biomedical Engineering Department, Faculty of Electrical Engineering, Iran University of Science and Technology (IUST), Narmak, Tehran 16846-13114, Iran

<sup>2</sup> School of Cognitive Sciences (SCS), Institute for Research in Fundamental Science (IPM), Niavaran, Tehran, Iran

<sup>3</sup> Department of Biopsychology, Institute of Cognitive Neuroscience, Faculty of Psychology, Ruhr-University Bochum, Bochum, Germany

<sup>4</sup> Radiology Department, AJA University of Medical Sciences, Tehran, Iran

manifestations of electrophysiological activities as the signature of neuronal communication during different mental task activities.

Neural coding in the brain is referred to the representation of applied stimuli or behavioral processing in electric potential difference at synapses and cell bodies of one or population of neurons [23]. Recorded scalp potential using EEG contains oscillatory signals that reflect the related effects to mental states such as object recognition, visual processing and decision making [16, 18, 42, 45]. Previous brain imaging studies have demonstrated that different spatial patterns of neural oscillations are associated with presenting different categories of objects (for example, animals, flowers and foods) [5, 9, 14, 31, 44]. The literature reported many studies that demonstrate the relation between power of oscillatory signals and sensory-cognitive processes, for example, by reporting correlations between object recognition and EEG signal power, sensory stimulus features [16, 18, 42, 45], but since EEG is stochastic signals, recent work from VanRullen et al. [44] focused on the dynamic signature of EEG signals. There is increasing evidence that the phase patterns of oscillation signals play a role in neural coding and can carry information about the mental task activity, but its importance during mental state information coding throughout the brain still need to be studied. Previous works have studied the precise temporal oscillations of EEG signals, and they have shown that the signal's phase can be informative for the sensory and cognitive task decoding [30, 34, 39, 44]. For example, Logothetis and his colleagues [34] demonstrated that the phase of the oscillation EEG signals can decode the auditory signals better than the power of oscillatory signals. Similarly, Montemurro et al. [32] found that when the information about the phase of oscillations affixed to neural decoding approaches, it increases the amount of information about the external stimulus as seen in the visual cortex. In high-level brain areas, it is possible that the phase coding utilized to a particular stimulus, for example, Siegel's study [41] about memorized objects in prefrontal cortex suggested that the phase of the gamma oscillation is thought to provide a framework for phase-dependent coding of memorized objects. Siegel et al. [25] found that in the temporal lobe, discrimination of correct/incorrect matches (card-matching task) based on the phase of oscillatory signals was significantly better than classification-based oscillation amplitude.

All of the above studies have tried to find a reasonable response to the questions of "which structures provide information that makes a suitable condition for single-trial classification of oscillation signals recorded from the brain?" and "how the phase coding occurs in cognitive processing [38]?". Some evidence from both human electroencephalogram (EEG) and nonhuman primate studies

suggested that when visual stimulus is presented to the subjects, the transient evoked potential that is modulated on top of an ongoing oscillation reflects the neural response [36, 40]. In contrast to the last evidences, some previous studies suggest that without an increase in amplitude, a reset of the phase has been detected in response to cognitive processes (spatial visual attention [27], auditory attention [24]). On the other hand, some studies demonstrated that both of increasing in oscillation amplitude and phase resetting had an effect on generation of event-related potentials during mental task activity [11]. The above evidences demonstrate that it is unknown how the mental task activity varies between brain regions for the same task. The interesting challenge in scientific committees is answering a reasonable response to the question: "Are different brain regions associated with different mechanism [25]?".

Here we investigate single-trial phase coding in five brain's lobes of the human brain (prefrontal, temporal, parietal, occipital and central lobes) using EEG recorded during an object categorization task. We assess the relevance of the oscillatory signals in object categorization task to phase coding and in addition, and we investigate two possible mechanisms of information coding (power/phase of oscillatory signal) associated with oscillatory signals in each brain lobe.

## 2 Materials and methods

### 2.1 Participants

The subjects who participated in the experiment were ten adults (two females, age between 18 and 28, one left hand, and the mean age of two females and eight male was 24 and 23 years, respectively). Before the experiment, they gave written informed consent prior to participation in the experiment. All participants had normal vision, and they reported that they did not suffer from any neurological or psychological disorder. The data of one subject were excluded because of the noise.

### 2.2 Visual stimulus

In this study, the visual stimulus presented across experiments contained 12 categories of different objects (animal, flower, body parts, etc.) in which each category consisted of five semi-sized (600 × 800 pixels) color images (Fig. 1a). Each subject had to participate in an experiment with 12 trials. The experiment for each subject has been recorded in two different sections with 3-min intersession interval to avoid of subject's mental fatigue. Each session contained 6 trials with 7-s inter-trial interval. At the beginning of each trial, the name of the target category (one of six categories)

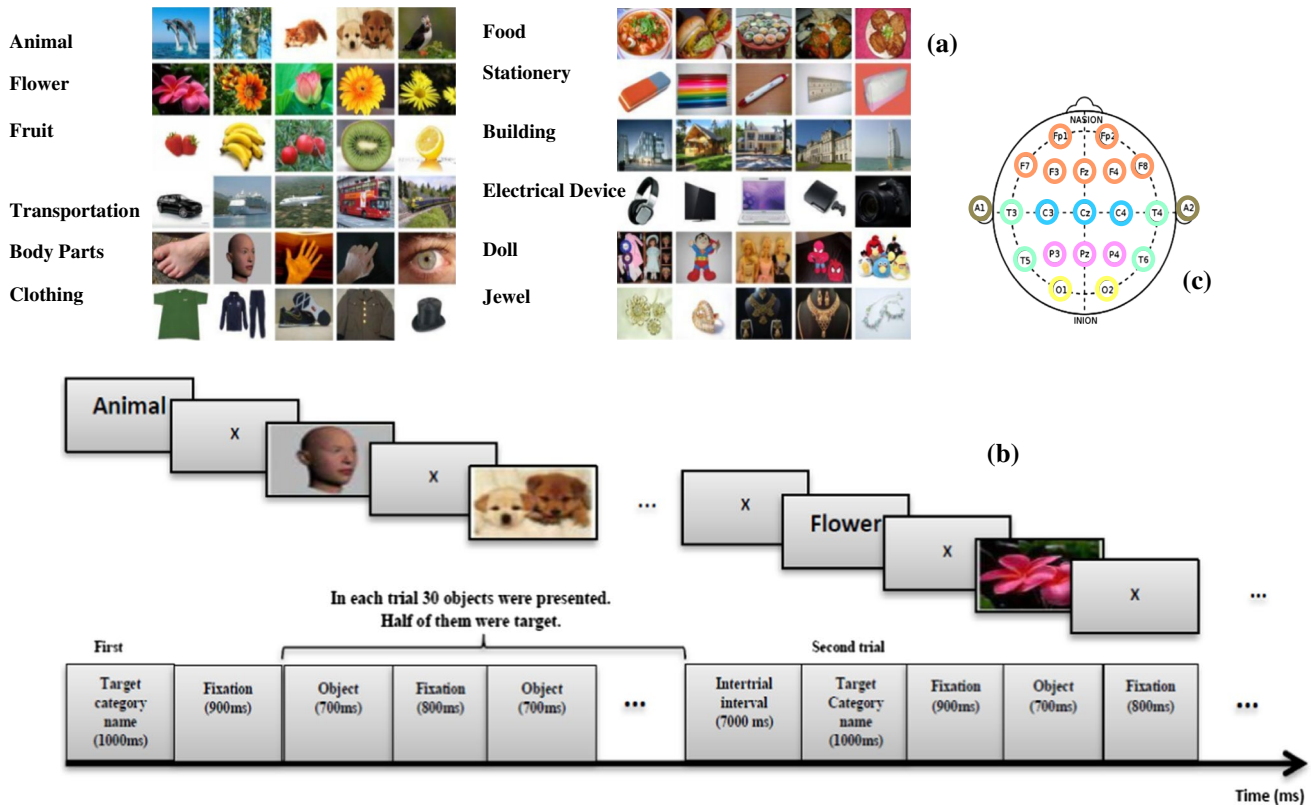


**Fig. 1** **a** Presented objects in the experiment. **b** Stimulus protocol. At the beginning of each trial, the name of target category was presented to the subjects (for 1 s) and they were asked to define which presented object consists of the target category. Subjects entered their answers by pressing the mouse left or right clicks (*left* correct, *right* false) which presented objects across trial were related to target category. Along each trial, 30 objects were presented (each one presented

for 700 ms) to the subjects in that half of them were targeted (each object of the target category was repeated 3 times, and the sequence of object presentation was random) and another 15 objects were distractor (were selected randomly from other categories). **c** EEG recording system. Each *color coding* defines an individual brain's lobe (frontal, central, parietal, occipital and temporal lobes) (color figure online)

was presented to the subjects (for one second) and they were asked to define which presented object belongs to the target category. Subjects entered their answers by pressing the mouse left or right clicks (left = correct, right = false) which presented objects across trial were related to target category. Along each trial, 30 objects were presented (each one presented for 700 ms) to the subjects in that half of them were targeted (each object of the target category was repeated three times, and the sequence of object presentation was random) and another 15 objects were distractor (were selected randomly from other categories). The stimulus presentation protocol is shown in Fig. 1b. The stimuli were designed using PSYTASK software (<http://psytask.software.informer.com/>).

### 2.3 Human EEG recordings and data preprocessing

Nineteen-channel EEG recording system was used to record brain signals (Fig. 1c). Each subject's EEG signals were continuously recorded from human scalp surface

according to the standard 10–20 system using Ag/AgCl electrodes placed on a Cap. The channels name which had recorded brain signals were, respectively, Fp1, Fp2, F3, F4, C3, C4, P3, P4, O1, O2, F7, F8, T3, T4, T5, T6, Fz, Cz and Pz. The reference electrodes were fixed at the subject's auricle (A1 and A2 channels). Electrode impedance was kept under 5 KΩ. The signals were amplified by a Mio-star amplifier (EEG-202 model) which was synchronized with the WINEEG software (<http://www.novatecheg.com/wineeg.html>). The EEG data which were recorded with 500-Hz sampling rate were filtered by a Hamming-windowed FIR band-pass filter of 0.1–150 Hz (the filter was designed using a MATLAB filter function).

Recorded EEG data were saved in EEG format, so we had to reformat the data to edf format to be readable in Matlab. Data were reformatted using WINEEG software from EEG format to edf format. Matlab software was used for preprocessing and post-processing of EEG data. The artifact criteria for individual trials contained the amplitude on any of the central, parietal, temporal and occipital channels (C3, Cz,

C4, P3, Pz, P4, T3, T4, T5, T6, O1, O2) upper than 7 standard deviations (SDs) of the signal. For subsequent analysis, we analyzed all channels individually and then we averaged the signals for those central, parietal, temporal, occipital and frontal channels to get a single signal for individual brain lobes. Data were filtered in individual bands (delta 1–4 Hz, theta 4–8 Hz, alpha 8–14 Hz, beta 14–20 Hz, gamma 20–30 Hz) using EEGLAB functions toolbox (filtfilt function, the 500-Hz recording was down-sampled to a sample rate of 256 Hz), and Hilbert transform was applied to calculate the signal phase and power [1]. Squared absolute value of Hilbert transform amplitude was considered as signal power.

The power of EEG signals was normalized (mean = 0, SD = 1) in an individual trial across time to equate the variation across time using the following equation:

$$x_{in} = \frac{x_i - \bar{x}}{\sigma} \tag{1}$$

where  $x_i$  is the  $i$ th time point in the power of EEG signals,  $\bar{x}$  is the mean of the features (EEG power in individual trial), and  $\sigma$  is the SD of individual trial.

### 2.4 Measure of inter-trial phase coherence

Phase coherence across trial of oscillatory phase was obtained for each time point  $t$  after trial onset by calculating the absolute value of the complex-valued of phase across trials:

$$IPC(t) = |\langle \exp(i \cdot \varphi(t)) \rangle|, \tag{2}$$

where  $pc(t)$  denotes time course of calculated phase coherence across trials,  $\varphi(t)$  indicates time course of considered signal on an individual trial,  $\langle \cdot \rangle$  is the trials average, and  $|\cdot|$  denotes the absolute value [33]. The phase coherence measures the phase variation across time of all trials.

### 2.5 Decoding analysis

This study wants to demonstrate how well various object categories could be discriminated from human brain signals, how long it would take to have enough information to identify objects category from EEG signal's parameter such as amplitude or phase, and which one of them has more information about object categories in the short time. We applied a decoding approach to set of objects that were categorized in 12 semantic categories (Fig. 1a). Each category contained five objects that were presented repeatedly three times in each trial, so we had 180 samples (12 (trial) × 5 (object) × 3 (times repeats) = 180 samples) for each subjects.

### 2.6 Classification procedure

In this study, we used machine learning methods to identify in single trial of EEG signals which of the twelve semantic

categories (Fig. 1a) were presented to participants. Here the classifier was trained to recognize the object category from evoked patterns from functional activities:

$$f : \text{EEG power or EEG phase} \rightarrow \text{object category(12 category)} \tag{3}$$

Prediction procedure was based on naïve Bayesian classification (NBC) [37]. In the machine learning, naïve Bayes classifier technique applies Bayes' theorem to discriminate the samples through high-dimensional independent feature spaces. Actually, naïve Bayesian classifier as a simple probabilistic classifier tries to parameterize the conditional probability model to elicit the posterior probability of input sample to predict the class which the input vector  $X (x_1, x_2, \dots, x_n)$  belongs to:

$$\text{Posterior} = \frac{\text{prior} \times \text{likelihood}}{\text{evidence}} \tag{4}$$

$$p(C_i|X) = p(X|C_i) \cdot \frac{p(C_i)}{p(X)} = \prod_{j=1}^n p(x_j|C_i) \cdot p(C_i) \tag{5}$$

where  $n$  is the number of features. The probabilities  $p(x_1|C_i), p(x_2|C_i), \dots, p(x_n|C_i)$  can be computed from the training set. For more information about the naïve Bayes classifier, readers can review the [10, 37].

Classification accuracy was used to evaluate the classifier accuracy. For achieving the classifier accuracy, the leave-one-out cross-validation procedure [22] was applied on the recorded brain activation data set. The decoding method was applied for the presented objects based on the individual repeat for each object (example data in Fig. 1a). We had 180 samples in features space, so we optimized NBC's parameter on training data set with 179 samples and the performance was tested with one remaining sample; we repeated this approach for 180 times, and then the average of 180 times was reported as decoding performance (the number of samples was not 180 in all subjects because of mistake, and the trials of incorrect behavioral task were ignored).

The mentioned procedure was applied (a) to the entire interval of 40–700-ms post-stimulus onset and (b) repeated again for small time bins, 2 ms, of duration of object presentation, and there was no overlap between small time intervals (330 intervals from 40 to 700 ms). This procedure was done to identify independent important data feature for each time interval.

After creating a predictive model, it is necessary to find out a measure of goodness. Most important measurement for evaluation of classifiers is an error (misclassification). Confusion matrix can make a full picture of the errors made by classification model. Different information about the classification can be extracted from confusion matrix: precision, sensitivity and specificity (for more information,

		Predicted Class		
		A	B	C
Actual Class	A	$TP_A$	$E_{AB}$	$E_{AC}$
	B	$E_{BA}$	$TP_B$	$E_{BC}$
	C	$E_{CA}$	$E_{CB}$	$TP_C$

$$Precision_A = \frac{TP_A}{TP_A + E_{BA} + E_{CA}}$$

$$Recall = Sensitivity_A = \frac{TP_A}{TP_A + E_{AB} + E_{AC}}$$

$$Specificity_A = \frac{TN_A}{TN_A + E_{BA} + E_{CA}}$$

$$TN_A = TP_B + E_{BC} + E_{CB} + TP_C$$

**Fig. 2** Mutli-class confusion matrix. Precision is a measure of the accuracy provided that a specific class has been predicted. Sensitivity is a measure of the ability of a classifier to select samples of a certain class from a data set. Specificity corresponds to the true-negative rate. TP and E are the number of true positive and false positive predictions for the considered class, respectively

readers can see our previous publication [3]). Figure 2 represents a short description of multi-class confusion matrix. Figure 3 depicts the strategy of analyzing the brain signals.

### 2.7 Statistical significance

The significance of prediction performance was evaluated using the statistical test (rank-sum test) [10]: We calculated the chance level performance for the decoding procedure with random labeling to the data. The random labeling was done 100 times to make a vector for the chance level performance. In different frequency bands and in the individual electrodes, the significance level was computed to define the significant time bins that have more information about the object categories. This approach was used to find the chance level and significance estimate for the predicting the object category using various parameters of EEG signals (phase and power of EEG signals).

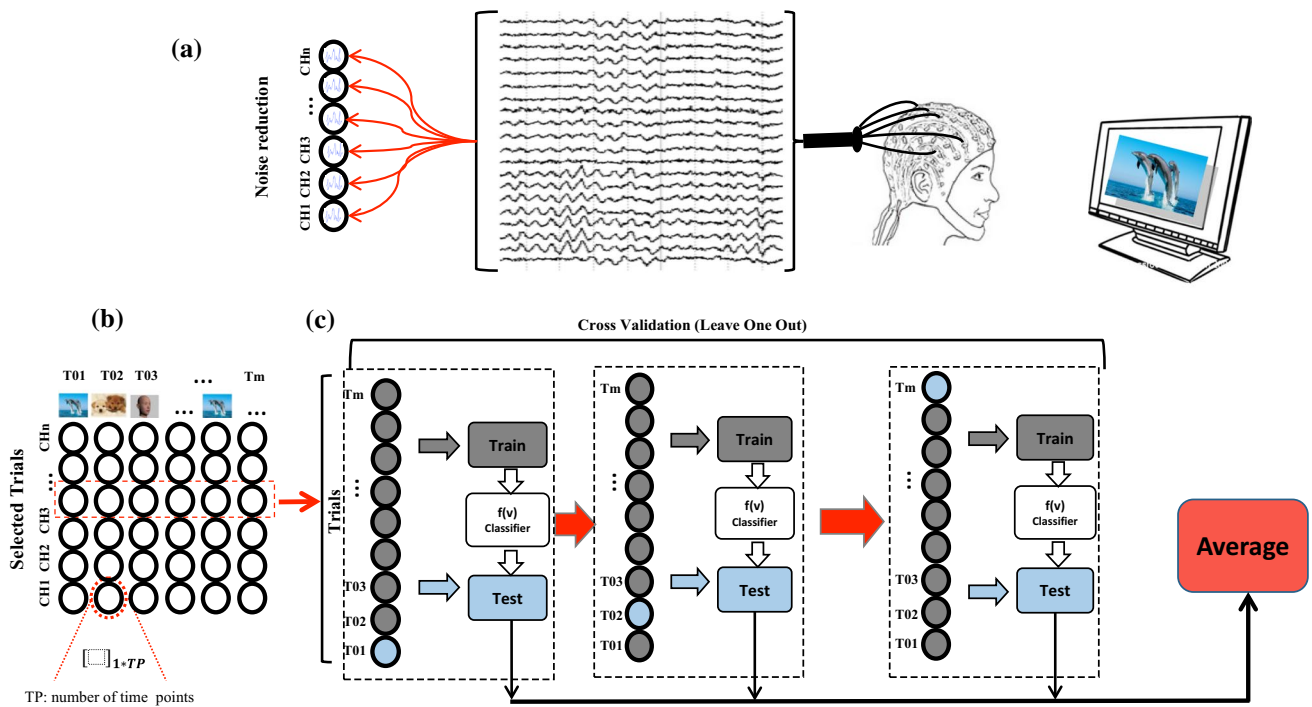
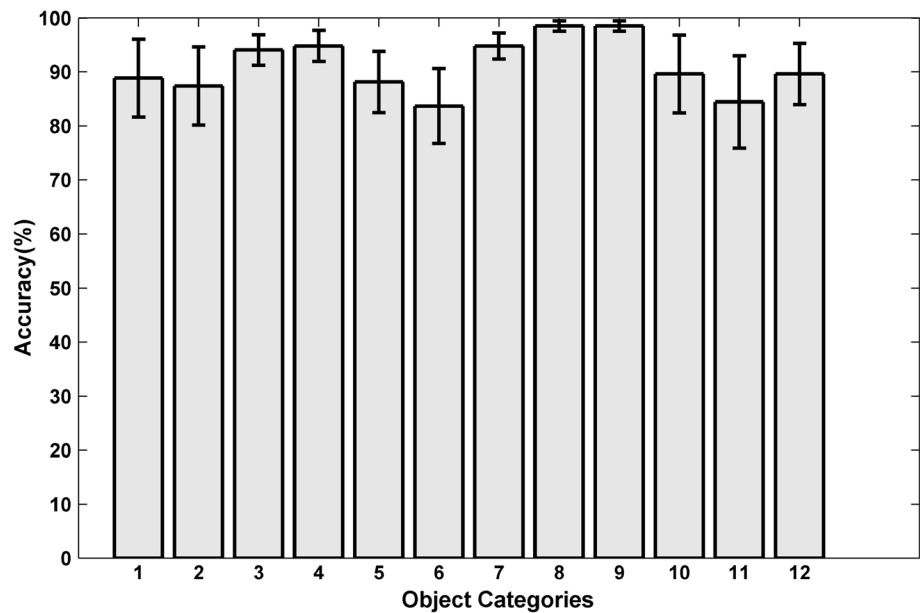


**Fig. 3** Illustration of the study and showing how the signals have been analyzed using statistical pattern recognition approach. **a** Viewing 60 objects from 12 categories (Fig. 1). A noise reduction procedure is done to determine which trials were avoided from analysis and which ones could be used in classification procedure. **b** The selected trials from individual electrodes are decomposed to the samples that correspond to the brain activation pattern during viewing of the special object. These samples are labeled based on the experimental condition (12 semantic categories of objects). **c** Naïve Bayesian classifier in combination with leave-one-out cross-validation is applied in discrete brain patterns to predict the presented object using

corresponding activated patterns. In leave-one-out cross-validation, the one sample is chosen as the test data and remaining samples of data as the training set. This procedure is repeated on all samples of the data set. The average of single classifications is reported as an accuracy of the classification. The mentioned classification step is repeated for two different feature spaces: (1) the feature space having the entire interval of 40–700-ms post-stimulus onsets, and (2) the feature space including the small time bins, 2 ms, of duration of object presentation with no overlap between small time intervals (330 intervals from 40 to 700 ms)

**Fig. 4** Behavioral analyses: On each trial, 30 objects were presented to participants in that half of them were targeted object. They were asked to press right mouse click when saw the target object. The *vertical axis* shows the accuracy of the subject's response to defining that the presented objects in each trial were related to the target category. The *horizontal axis* shows the various categories of objects that were presented in this study (animals, food, flower, etc.)



### 3 Results

We recorded brain response to present objects as a block design stimulus sequence consisting of 60 objects in 12 semantic categories such as animal, flower, food, etc. (Figure 1a). These images provided a rich and dynamic stimulus that covered a wide range of objects in natural surroundings and which evoked a robust and dynamic signature in frequency scalp. In this study, to compare the selectivity of object categories in oscillatory brain signals, we used a framework of stimulus decoding. Such predicting analysis method quantifies how a set of sensory inputs (presented object categories) can be predicted by recorded single-trial responses and provides a measure of signal selectivity with respect to the sensory input. In each trial, we sampled first 660 ms (the time interval of 40 ms from the picture onset was removed) of stimulus presented during the actual experiment in individual trial and then we applied the decoding analysis method to brain oscillatory signals in individual trials. In the following, we first demonstrated single-trial classification results from the oscillation power and phase. We subsequently demonstrate how the selectivity of the phase of low frequency of EEG signals is significantly greater than the power of slow oscillations. In contrast, the selectivity of the power of high oscillations is significantly greater than the phase of high oscillations.

#### 3.1 Behavioral analysis

The first step is studying behavioral responses of subjects to demonstrate the data authentication. So, we analyzed the behavioral response, and we demonstrated that each category can be classified by subject with high accuracy with

respect to chance level (because we presented 12 semantic categories, chance level accuracy is 8.33 %) (Fig. 4).

#### 3.2 Identifying object categories using power and phase of EEG signal

We recorded EEG oscillation signals from 10 volunteers who performed an object categorization task (Fig. 1b) while watching the color images of objects (the data of one subject is ignored). For each participant, the 19-channel EEG system (Fig. 1c) records brain signals across the semantic object categorization task. Here, we focused on correct response and in subsequential analysis only used this set of EEG recorded data. The recorded EEG data were filtered in various frequency bands (delta 1–4 Hz, theta 4–8 Hz, alpha 8–14 Hz, beta 14–20 Hz, gamma 20–30 Hz) and the power and phase of signals in a different frequency bands calculated using Hilbert transform.

In the first analysis, inter-trial phase coherence was calculated in all brain lobes [F (frontal lobe), C (central lobe), P (parietal lobe), T (temporal lobe) and O (occipital lobe)], and it was highest over temporal lobe electrodes and strongest in the delta (1–4 Hz) frequency band (median 0.1631, randomization test  $p < 0.001$ , Fig. 5). This temporal and frontal localization of object-entrained is in good concordance with the our last study using fMRI [3]. Our last study demonstrated that the frontal, temporal and fusiform regions are informative in object categorization task.

In the second analysis, oscillations of EEG signal were analyzed using the NBC decoding method to identify the stimulus selectivity of recorded EEG signals during viewing image of semantic object categories. The power and phase of the entire interval of 40–700 ms

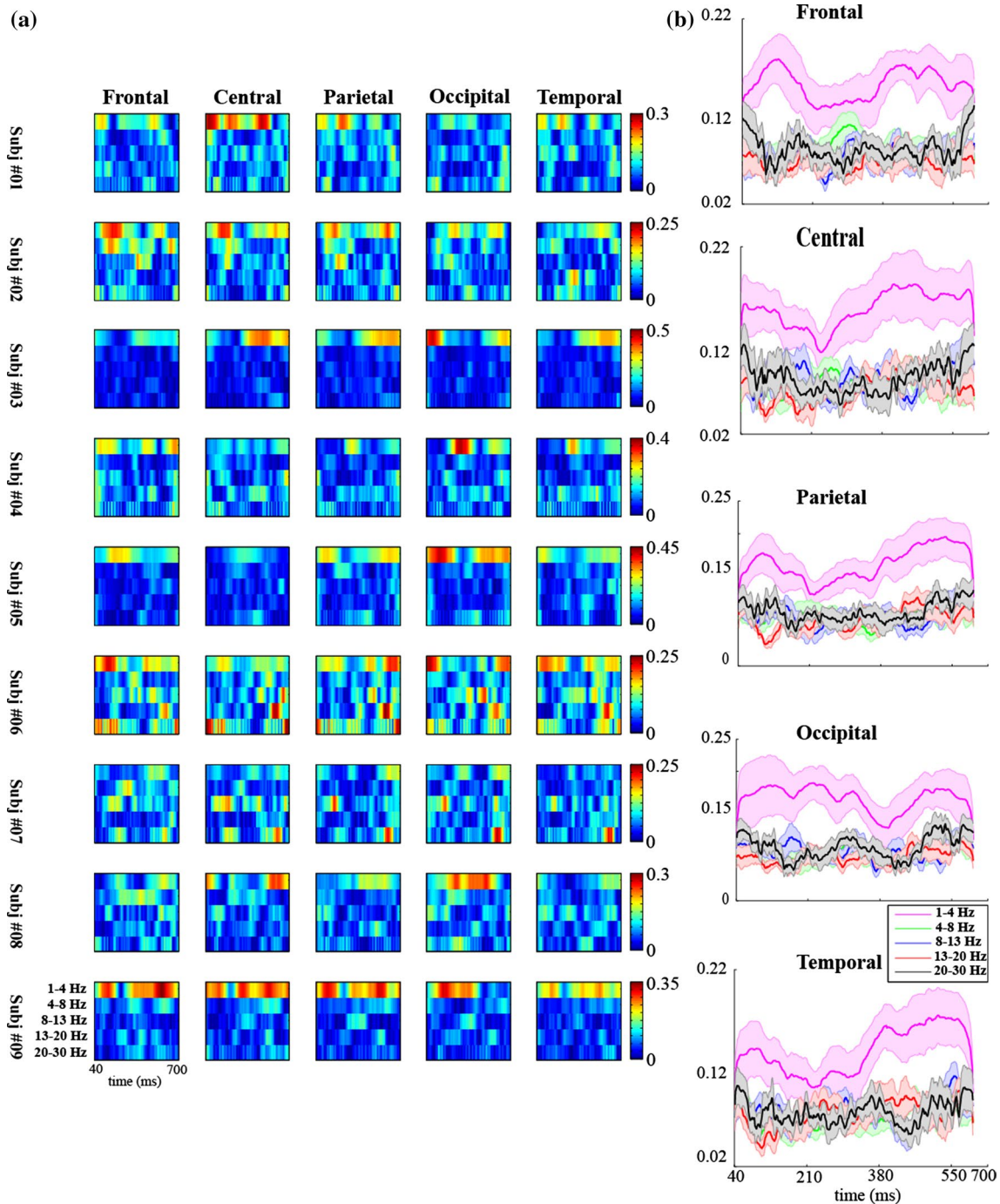


**Fig. 5** **a** Inter-trial phase coherence across different frequency bands in five brain regions. **b** Mean of inter-trial phase coherence across subjects in a different brain region in various frequency bands

post-stimulus onset in a different frequency band of the oscillation signal were applied as features in decoding stage. Figure 6 illustrates the power and phase of all trials for a sample subject from the object stimulus (660-ms duration). Clearly, the phase of the oscillation signals in different brain areas is more consistent across trial with respect to the power of the collected signals, reflecting

the entertainment of the oscillatory dynamics of the object stimulus (color coding illustrates the consistent phase across trial, Fig. 6). In this step, 19 electrodes were investigated independently. An NBC algorithm was applied to the collected single-trial oscillatory responses from different brain regions across object categorization task to predict the object category. Figure 7 illustrates

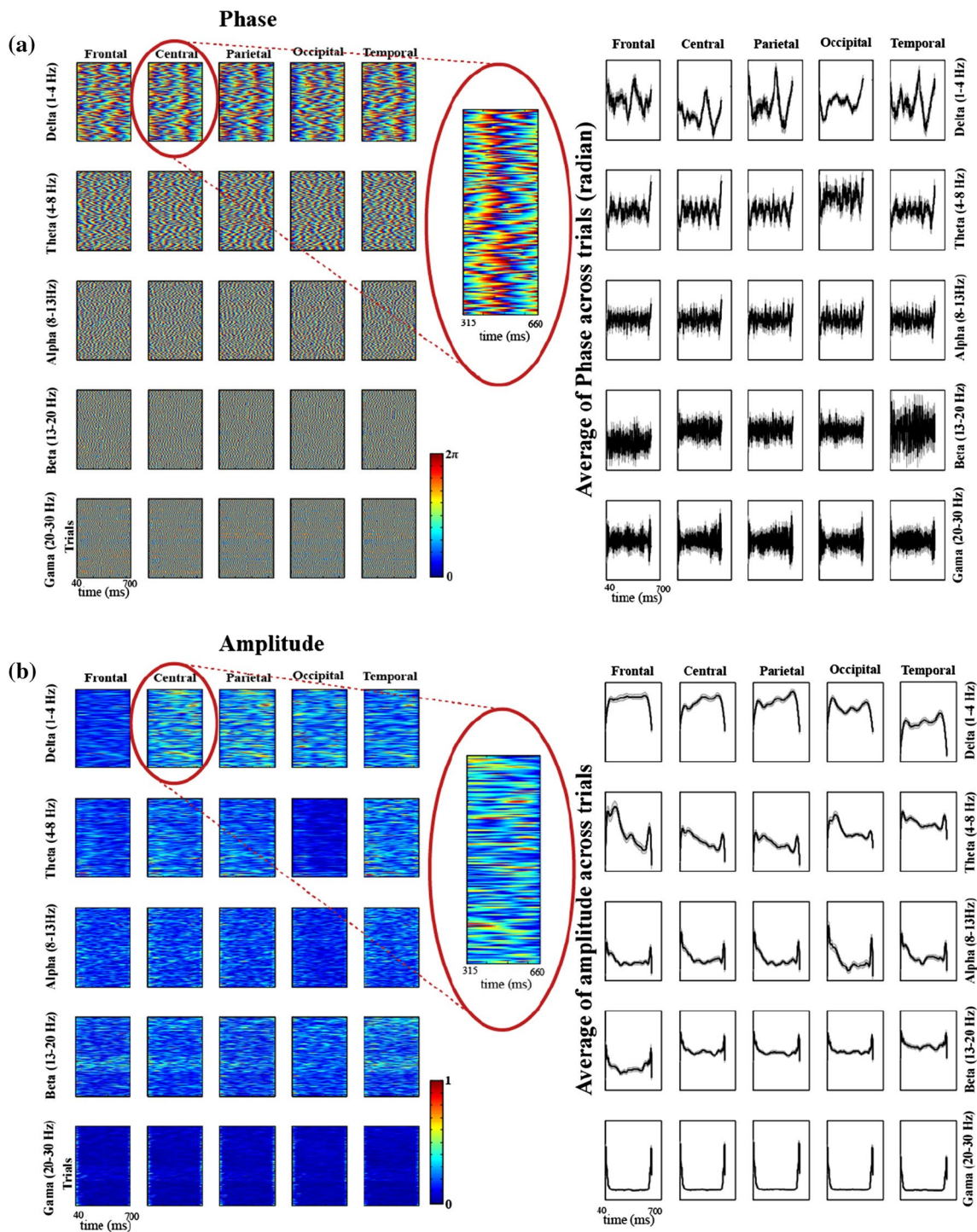


**Fig. 6 a** Example data of the different frequency band’s power and phase across multiple trials during the presentation of objects’ images. This figure reveals a higher reliability of the phase value across trials, visible as a better alignment of the same signal values

(color code) across trials for phase. **b** Average of the phase and power of trials in all frequency bands. Shaded bar indicated the SE of mean (color figure online)

the pattern of decoding performance using EEG oscillation power and phase in different frequency bands across whole brain regions. Decoding results demonstrated a measure for evaluating the amount of information in

recorded brain signals from single electrodes which was related to the categorization task. As shown in Fig. 7, the phase of oscillation signals was informative in low-frequency band, while the power of high-frequency band

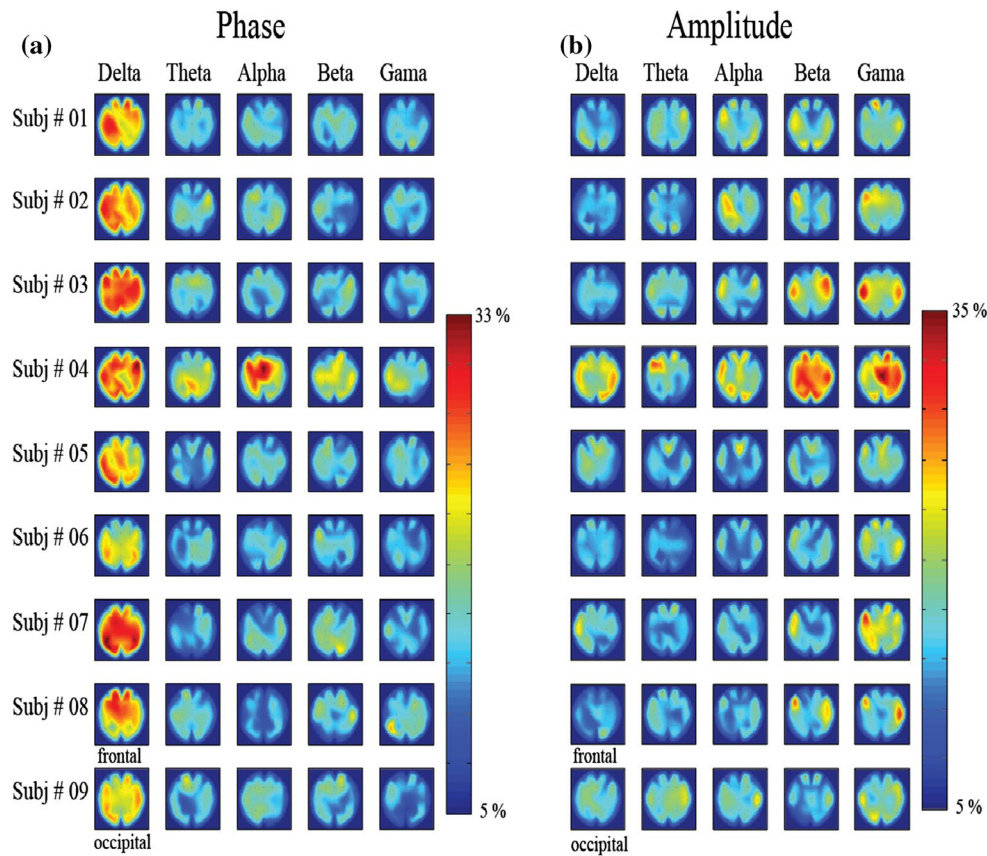


**Fig. 7** Decoding patterns. **a** Phase decoding; here each electrode is investigated separately. **b** Amplitude decoding across the region of interest. Color code demonstrates the accuracy of NB classifier as a measure of information (color figure online)

was informative with respect to the phase of this band. Figure 7 suggests that which electrodes are informative about an object categorization task. The informative brain activation signals were localized in frontal, centro-parietal and occipito-temporal electrodes (Fig. 7a) when the feature in feature space is a phase. The relevant data feature about object categorization was located in the occipito-temporal and fronto-temporal electrodes (Fig. 7b) when the classifier feature space is a power of EEG signals.

In the third analysis, we tried to demonstrate how the information about object categories represented on brain activation signals across the time, and we divided the trial into sort time bins (2 ms) and evaluated the NB classifier on these bins independently. In this step, we divided the brain into five regions frontal, temporal, central, parietal and occipital lobes and averaged the EEG electrodes in each region of interest independently and then applied NB classifier for each time bin. The results demonstrate the importance maps for object categorization in that the decoding accuracy across the time was not significant in all the time in all brain regions and yielded the poor performances in sometimes (Fig. 8).

As shown in Fig. 8, the decoding accuracy across different frequency bands in five brain regions was considerably significant when the phase of low frequency of the oscillatory signal was interested feature; in contrast, decoding accuracy based on power of high frequency is considerably significant across the time. The statistical test (rank-sum test) demonstrated the significance for the decoding from phase of low-frequency band ( $p < 0.001$ , 1–4 and 4–8 Hz) and the power of high-frequency band ( $p < 0.001$ , 20–30 Hz). For evaluating the classification model, we represent precision and sensitivity percentages in Tables 1 and 2.

### 3.3 Classification performance in brain lobes is associated with transient increase in inter-trial phase coherence (IPC)

The results presented so far have demonstrated that the discrimination between different object categories is possible using the single-trial phase of the EEG oscillatory signals. This result refers that the phase across trials of oscillatory signals has a certain amount of consistency in the information about the object's category.

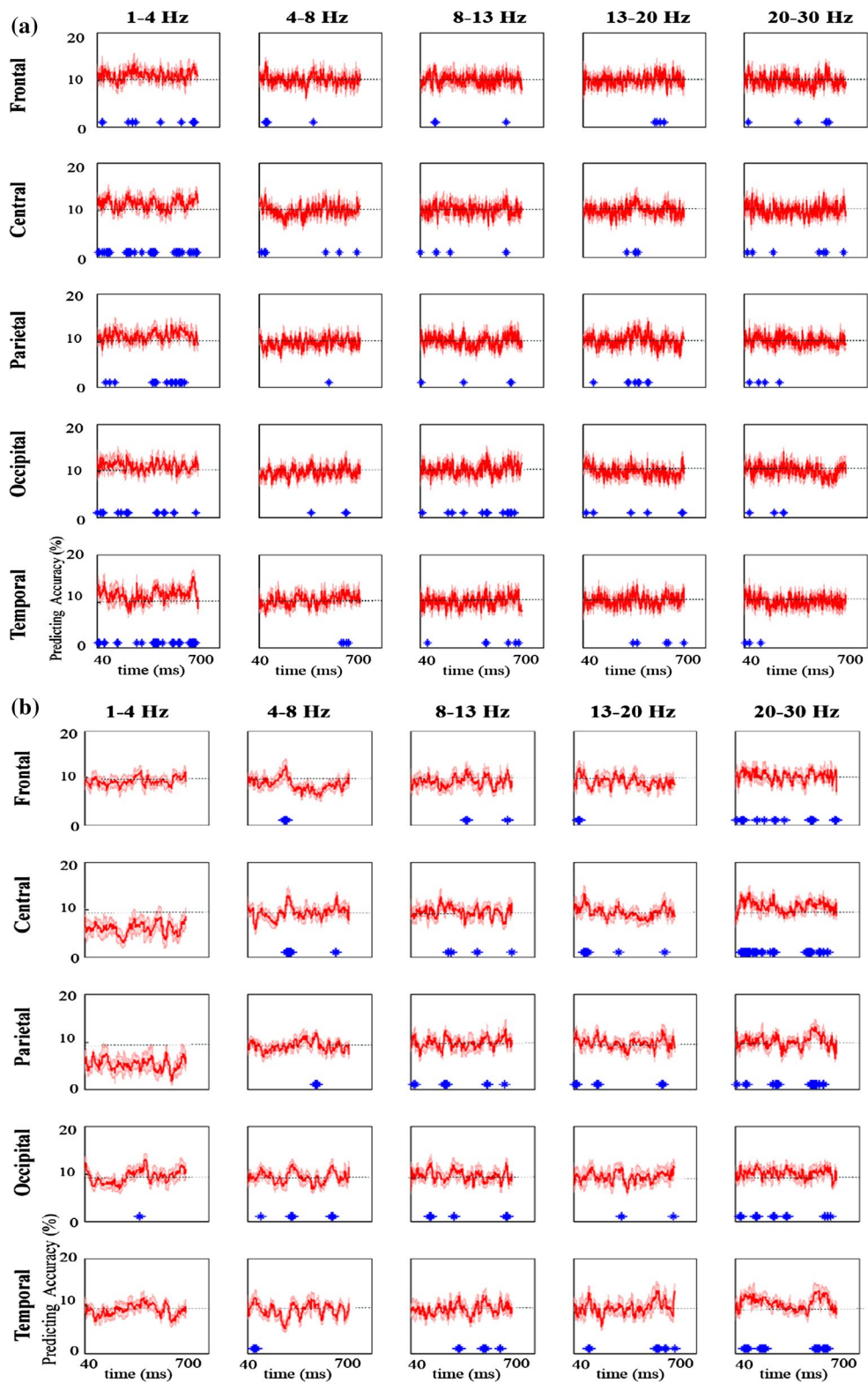


**Fig. 8** **a** Decoding accuracy across the time when the considered features are the angle of the EEG signal. **b** Decoding accuracy across the time when the considered features are the power of the EEG signal.

The *dash line* is the chance level. The *shadow* represents the deviation from mean across subjects

**Table 1** Evaluation measures in the confusion matrix when the phase of delta band of EEG signals is considered feature

Electrodes	C1	C2	C3	C4	C5	C6	C7	C8	C9	C10	C11	C12
E1												
P	0.23	0.24	0.28	0.16	0.24	0.16	0.3	0.35	0.2	0.26	0.3	0.33
R	0.21	0.2	0.2	0.18	0.21	0.16	0.26	0.48	0.19	0.19	0.35	0.29
S	0.85	0.86	0.86	0.83	0.86	0.84	0.81	0.81	0.84	0.84	0.85	0.86
E2												
P	0.34	0.22	0.18	0.22	0.26	0.14	0.22	0.34	0.17	0.27	0.34	0.29
R	0.27	0.18	0.16	0.15	0.28	0.16	0.22	0.43	0.19	0.21	0.43	0.29
S	0.87	0.87	0.85	0.87	0.85	0.85	0.83	0.82	0.82	0.85	0.85	0.86
E3												
P	0.32	0.18	0.22	0.3	0.15	0.07	0.34	0.32	0.19	0.30	0.37	0.29
R	0.29	0.21	0.16	0.22	0.12	0.1	0.46	0.39	0.16	0.28	0.45	0.25
S	0.86	0.84	0.86	0.86	0.86	0.85	0.82	0.81	0.85	0.86	0.86	0.84
E4												
P	0.24	0.23	0.18	0.33	0.19	0.18	0.34	0.36	0.2	0.19	0.33	0.26
R	0.13	0.19	0.18	0.18	0.18	0.16	0.41	0.43	0.19	0.24	0.4	0.35
S	0.86	0.86	0.85	0.85	0.86	0.86	0.82	0.82	0.85	0.84	0.85	0.82
E5												
P	0.37	0.29	0.11	0.35	0.26	0.21	0.39	0.43	0.25	0.28	0.27	0.244
R	0.4	0.37	0.1	0.28	0.2	0.19	0.45	0.45	0.25	0.28	0.29	0.27
S	0.85	0.85	0.85	0.85	0.85	0.86	0.82	0.83	0.84	0.86	0.86	0.84
E6												
P	0.36	0.19	0.21	0.23	0.2	0.16	0.29	0.48	0.17	0.25	0.19	0.32
R	0.47	0.19	0.16	0.21	0.19	0.19	0.32	0.47	0.16	0.23	0.22	0.43
S	0.84	0.86	0.86	0.85	0.86	0.85	0.83	0.84	0.84	0.86	0.86	0.83
E7												
P	0.38	0.21	0.24	0.24	0.28	0.1	0.34	0.35	0.19	0.29	0.21	0.16
R	0.27	0.19	0.2	0.18	0.27	0.13	0.49	0.76	0.19	0.3	0.24	0.2
S	0.87	0.86	0.85	0.86	0.86	0.85	0.82	0.82	0.84	0.85	0.86	0.83
E8												
P	0.37	0.23	0.16	0.2	0.2	0.2	0.28	0.26	0.17	0.31	0.2	0.21
R	0.37	0.21	0.16	0.19	0.21	0.2	0.29	0.26	0.15	0.28	0.24	0.24
S	0.86	0.86	0.84	0.84	0.84	0.85	0.84	0.83	0.84	0.86	0.84	0.83
E9												
P	0.21	0.09	0.23	0.33	0.35	0.15	0.26	0.31	0.25	0.24	0.19	0.19
R	0.2	0.1	0.23	0.29	0.37	0.11	0.29	0.35	0.23	0.3	0.2	0.23
S	0.86	0.86	0.84	0.84	0.84	0.85	0.84	0.83	0.84	0.86	0.84	0.83
E10												
P	0.29	0.12	0.25	0.27	0.2	0.15	0.23	0.31	0.18	0.29	0.15	0.18
R	0.2	0.16	0.26	0.21	0.2	0.19	0.22	0.33	0.2	0.32	0.16	0.18
S	0.87	0.85	0.84	0.85	0.86	0.85	0.84	0.84	0.82	0.85	0.85	0.83
E11												
P	0.21	0.2	0.19	0.27	0.17	0.21	0.27	0.29	0.18	0.23	0.33	0.2
R	0.2	0.16	0.18	0.27	0.19	0.23	0.29	0.37	0.16	0.26	0.32	0.21
S	0.85	0.87	0.86	0.83	0.84	0.84	0.84	0.81	0.85	0.84	0.87	0.84
E12												
P	0.14	0.21	0.29	0.21	0.22	0.16	0.27	0.26	0.21	0.19	0.21	0.24
R	0.16	0.19	0.29	0.16	0.19	0.18	0.27	0.29	0.16	0.22	0.23	0.33
S	0.86	0.86	0.84	0.85	0.86	0.84	0.84	0.83	0.85	0.84	0.84	0.81
E13												
P	0.25	0.21	0.18	0.27	0.17	0.1	0.32	0.38	0.23	0.32	0.25	0.21

**Table 1** continued

Electrodes	C1	C2	C3	C4	C5	C6	C7	C8	C9	C10	C11	C12
R	0.25	0.21	0.15	0.24	0.19	0.1	0.37	0.44	0.23	0.26	0.26	0.25
S	0.85	0.86	0.86	0.84	0.84	0.86	0.83	0.83	0.83	0.87	0.86	0.83
E14												
P	0.23	0.1	0.21	0.28	0.1	0.19	0.29	0.27	0.17	0.23	0.2	0.28
R	0.25	0.1	0.2	0.26	0.1	0.18	0.32	0.24	0.1	0.2	0.24	0.41
S	0.86	0.86	0.85	0.85	0.86	0.83	0.83	0.84	0.86	0.87	0.84	0.82
E15												
P	0.27	0.1	0.21	0.28	0.17	0.16	0.45	0.36	0.2	0.34	0.26	0.22
R	0.2	0.2	0.2	0.19	0.2	0.2	0.67	0.43	0.2	0.3	0.27	0.27
S	0.86	0.85	0.87	0.86	0.84	0.84	0.81	0.82	0.85	0.87	0.86	0.83
E16												
P	0.18	0.22	0.23	0.20	0.16	0.19	0.29	0.37	0.22	0.26	0.18	0.27
R	0.19	0.19	0.2	0.21	0.19	0.21	0.35	0.31	0.22	0.25	0.19	0.3
S	0.86	0.87	0.85	0.83	0.85	0.84	0.83	0.85	0.83	0.86	0.85	0.84
E17												
P	0.28	0.25	0.19	0.27	0.18	0.11	0.33	0.38	0.2	0.24	0.38	0.24
R	0.28	0.24	0.16	0.22	0.19	0.17	0.47	0.44	0.18	0.26	0.37	0.22
S	0.85	0.86	0.86	0.86	0.86	0.85	0.81	0.82	0.85	0.85	0.86	0.85
E18												
P	0.33	0.27	0.16	0.27	0.16	0.14	0.28	0.37	0.20	0.24	0.39	0.21
R	0.39	0.27	0.16	0.25	0.13	0.1	0.42	0.4	0.19	0.27	0.4	0.2
S	0.85	0.86	0.85	0.84	0.87	0.87	0.82	0.83	0.84	0.85	0.86	0.84
E19												
P	0.42	0.23	0.25	0.22	0.19	0.25	0.32	0.26	0.2	0.35	0.23	0.19
R	0.38	0.2	0.22	0.2	0.21	0.25	0.4	0.28	0.19	0.33	0.32	0.2
S	0.87	0.87	0.85	0.85	0.85	0.86	0.82	0.82	0.83	0.86	0.84	0.85

The values are average over all nine subjects

*P* precision, *R* recall, *S* specificity, *C* category

The inter-trial phase coherence (IPC) is a measure that we can use it to show this consistency across the phase of single trials: At the certain time point, a uniform distribution of phase across trial is determined by zero value of IPC, and the same phase across all trials is determined by the value of one [26]. Figure 5 shows the IPC based on phase on different frequency bands across different brain regions. Figure 5 represents that IPC in low-frequency band of oscillatory signals has the highest amount with respect to IPC in other frequency bands. For studying the relationship between IPC and decoding pattern across the time (duration of object presentation), we calculate the cross-collation between IPC and decoding pattern from phase (Tables 3, 4). The results suggest that there is a positive correlation between IPC and decoding from phase in 1–4-Hz frequency band at parietal and temporal lobes. In contrast, there is a negative correlation between IPC and the decoding pattern in the 1–4-Hz frequency band at frontal and central lobes. But there is no any significant correlation in the occipital area.

## 4 Discussion

In this study, by using surface brain signals recording technology, we were able to investigate the phenomena of phase and power coding in different brain regions by using human EEG recordings. First, our results provides powerful evidence that the phase of oscillatory signals is a key element in information processing in a different brain regions across the low-frequency band (delta band, 1–4 Hz), and the information about the semantic category is encoded in the power of high-frequency band (gamma band, 20–30 Hz) (Figs. 7, 8). Second, we reported that the inter-trial phase coherence is significantly correlated to the pattern of EEG phase decoding during the time (Tables 3, 4).

### 4.1 Coding of cognitive states using oscillation phase

In this study, we investigate the possibility for predicting of semantic category of objects from single trial of oscillatory EEG signals. Our stimuli in this study were a set of five exemplars from 12 different semantic categories (Fig. 1)

**Table 2** Evaluation measures in the confusion matrix when the power of gamma band of EEG signals is considered feature

Electrodes	C1	C2	C3	C4	C5	C6	C7	C8	C9	C10	C11	C12
E1												
P	0.4	0.31	0.26	0.21	0.15	0.38	0.5	0.1	0.26	0.31	0.18	0.24
R	0.48	0.4	0.26	0.18	0.15	0.31	0.69	0.1	0.24	0.36	0.15	0.2
S	0.85	0.84	0.84	0.85	0.85	0.87	0.83	0.84	0.84	0.84	0.88	0.86
E2												
P	0.28	0.29	0.32	0.25	0.33	0.20	0.37	0.34	0.27	0.25	0.36	0.28
R	0.25	0.3	0.33	0.22	0.25	0.19	0.4	0.31	0.25	0.2	0.37	0.31
S	0.86	0.84	0.83	0.84	0.87	0.86	0.83	0.84	0.83	0.86	0.86	0.84
E3												
P	0.35	0.18	0.35	0.18	0.29	0.33	0.29	0.15	0.25	0.22	0.42	0.18
R	0.36	0.15	0.3	0.2	0.29	0.3	0.33	0.2	0.27	0.25	0.44	0.18
S	0.86	0.87	0.85	0.84	0.85	0.86	0.83	0.83	0.82	0.83	0.86	0.86
E4												
P	0.31	0.25	0.35	0.29	0.23	0.29	0.31	0.23	0.31	0.19	0.45	0.26
R	0.37	0.25	0.28	0.21	0.22	0.31	0.33	0.27	0.25	0.18	0.47	0.28
S	0.85	0.86	0.86	0.86	0.84	0.86	0.84	0.81	0.85	0.85	0.87	0.84
E5												
P	0.39	0.21	0.40	0.31	0.20	0.20	0.31	0.23	0.25	0.33	0.45	0.21
R	0.4	0.17	0.33	0.38	0.18	0.22	0.32	0.2	0.21	0.42	0.5	0.23
S	0.86	0.87	0.86	0.83	0.85	0.85	0.84	0.84	0.84	0.84	0.86	0.84
E6												
P	0.31	0.25	0.33	0.41	0.29	0.27	0.40	0.32	0.30	0.21	0.29	0.22
R	0.32	0.21	0.32	0.39	0.32	0.29	0.42	0.32	0.25	0.22	0.36	0.2
S	0.86	0.87	0.85	0.85	0.84	0.85	0.84	0.83	0.85	0.85	0.85	0.85
E7												
P	0.37	0.29	0.28	0.27	0.18	0.31	0.28	0.23	0.27	0.26	0.35	0.36
R	0.4	0.26	0.22	0.28	0.17	0.26	0.25	0.2	0.26	0.36	0.32	0.45
S	0.86	0.86	0.85	0.83	0.85	0.87	0.85	0.85	0.83	0.82	0.87	0.83
E8												
P	0.28	0.27	0.38	0.29	0.24	0.21	0.23	0.34	0.21	0.16	0.28	0.27
R	0.28	0.26	0.3	0.3	0.25	0.25	0.2	0.33	0.2	0.2	0.31	0.28
S	0.86	0.87	0.86	0.84	0.85	0.85	0.84	0.84	0.84	0.84	0.86	0.84
E9												
P	0.33	0.27	0.25	0.25	0.20	0.29	0.37	0.38	0.32	0.22	0.23	0.32
R	0.31	0.28	0.2	0.2	0.2	0.33	0.31	0.36	0.27	0.29	0.25	0.36
S	0.86	0.86	0.86	0.85	0.84	0.84	0.85	0.84	0.84	0.83	0.86	0.84
E10												
P	0.28	0.31	0.37	0.23	0.19	0.17	0.27	0.27	0.20	0.10	0.31	0.29
R	0.28	0.36	0.36	0.2	0.17	0.2	0.27	0.22	0.18	0.1	0.31	0.36
S	0.86	0.85	0.85	0.85	0.86	0.84	0.84	0.84	0.84	0.84	0.87	0.83
E11												
P	0.33	0.44	0.38	0.32	0.36	0.4	0.55	0.32	0.31	0.18	0.40	0.40
R	0.32	0.45	0.4	0.33	0.37	0.33	0.65	0.36	0.27	0.18	0.4	0.38
S	0.86	0.86	0.84	0.84	0.85	0.87	0.83	0.82	0.84	0.86	0.87	0.86
E12												
P	0.32	0.43	0.22	0.33	0.17	0.25	0.35	0.3	0.25	0.25	0.3	0.28
R	0.3	0.61	0.18	0.32	0.2	0.24	0.38	0.25	0.25	0.25	0.33	0.24
S	0.86	0.83	0.85	0.85	0.85	0.86	0.84	0.85	0.83	0.85	0.86	0.86
E13												
P	0.47	0.33	0.4	0.26	0.40	0.32	0.38	0.27	0.22	0.29	0.49	0.16

**Table 2** continued

Electrodes	C1	C2	C3	C4	C5	C6	C7	C8	C9	C10	C11	C12
R	0.56	0.28	0.28	0.2	0.4	0.33	0.4	0.28	0.16	0.24	0.64	0.2
S	0.85	0.87	0.87	0.85	0.85	0.85	0.83	0.83	0.86	0.86	0.85	0.83
E14												
P	0.48	0.38	0.42	0.42	0.49	0.32	0.46	0.28	0.32	0.25	0.42	0.39
R	0.51	0.44	0.36	0.41	0.41	0.33	0.44	0.27	0.31	0.25	0.45	0.28
S	0.85	0.85	0.86	0.85	0.87	0.85	0.85	0.83	0.84	0.85	0.86	0.87
E15												
P	0.25	0.24	0.36	0.21	0.16	0.38	0.25	0.35	0.27	0.22	0.27	0.30
R	0.27	0.27	0.31	0.2	0.16	0.45	0.21	0.29	0.27	0.22	0.29	0.36
S	0.85	0.85	0.5	0.84	0.86	0.85	0.85	0.85	0.83	0.86	0.85	0.84
E16												
P	0.27	0.33	0.38	0.33	0.23	0.27	0.25	0.32	0.29	0.2	0.27	0.33
R	0.27	0.31	0.36	0.27	0.2	0.33	0.24	0.32	0.25	0.25	0.23	0.38
S	0.85	0.87	0.85	0.85	0.85	0.84	0.85	0.83	0.84	0.84	0.87	0.84
E17												
P	0.47	0.27	0.41	0.30	0.20	0.27	0.39	0.26	0.27	0.36	0.44	0.21
R	0.44	0.21	0.33	0.28	0.2	0.27	0.48	0.25	0.29	0.38	0.5	0.2
S	0.87	0.87	0.86	0.84	0.84	0.86	0.83	0.83	0.83	0.85	0.86	0.86
E18												
P	0.4	0.22	0.37	0.33	0.26	0.23	0.37	0.36	0.33	0.37	0.40	0.24
R	0.4	0.2	0.3	0.33	0.3	0.22	0.33	0.27	0.27	0.37	0.46	0.27
S	0.86	0.86	0.86	0.84	0.84	0.86	0.85	0.85	0.84	0.83	0.86	0.84
E19												
P	0.33	0.3	0.3	0.33	0.21	0.12	0.31	0.38	0.22	0.26	0.23	0.26
R	0.33	0.3	0.22	0.37	0.2	0.16	0.25	0.27	0.2	0.36	0.25	0.28
S	0.86	0.86	0.86	0.83	0.85	0.86	0.85	0.85	0.86	0.83	0.85	0.85

The values are average over all nine subjects

*P* precision, *R* recall, *S* specificity, *C* category

**Table 3** Correlation coefficient between inter-trial phase coherence and performance of decoding from phase oscillations

	1–4 Hz	4–8 Hz	8–13 Hz	13–20 Hz	20–30 Hz
Frontal	<b>-0.3367</b>	<b>-0.2791</b>	0.0462	0.0400	0.0328
Central	<b>-0.1241</b>	-0.0239	-0.0650	0.0736	<b>0.3046</b>
Parietal	<b>0.3005</b>	-0.0039	<b>0.2296</b>	<b>-0.1681</b>	-0.0128
Occipital	-0.0999	-0.0423	0.0393	-0.0967	-0.0562
Temporal	<b>0.4929</b>	<b>0.1514</b>	<b>0.1708</b>	-0.0911	0.0665

Bold values represent the significant correlation between inter-trial phase coherence and performance of decoding

which presented for three times. Since naïve Bayes classifier is based on applying Bayes theorem, we assume that the features are strongly (naive) independent, and so it was applied for analysis.

The results of our work reveal that the phase of low frequency and power of high frequency of oscillatory signals have the same trends in representing the information

**Table 4** *p* value of correlation between IPC and decoding from phase in a different frequency bands and various brain regions

	1–4 Hz	4–8 Hz	8–13 Hz	13–20 Hz	20–30 Hz
Frontal	3.5e-10	2.56e-07	0.4030	0.4689	0.5530
Central	0.0241	0.6656	0.2391	0.1822	1.63e-08
Parietal	2.6e-08	0.9432	2.53e-05	0.0022	0.8169
Occipital	0.0698	0.4437	0.4767	0.0795	0.3083
Temporal	1.4e-21	0.0059	0.0018	0.0984	0.2284

of semantic categories. The phase of ongoing oscillation reflects related activity patterns to specific stimuli, and the reflected sensory information for coding the individual neural response during a behavioral task by slow oscillation is greater in their exact timing (phase) compared with an amplitude of oscillatory signals (power) [9, 21, 25, 32, 35]. The phase of our recorded data from the human scalp surface during object categorization tasks is in agreement with this finding, and our results suggest that the phase

of oscillatory signals plays a important role in coding of the behavioral task on stimulus-specific brain activity patterns.

The topographical representation of decoding accuracy indicates that in decoding from phase informative electrodes were localized in frontal, centro-parietal and occipito-temporal electrodes (Fig. 7a) and in decoding from power, the relevant data feature about object categorization were located in the occipito-temporal and fronto-temporal electrodes (Fig. 7b). This is in accordance with the most recent study by Gruber et al. [13], which demonstrated that the source of synchronized oscillatory gamma band activity (>20 Hz) during object categorization task arose from lateral occipito-temporal and inferior temporal cortical area.

There are a large number of neuroimaging studies that provided evidence for involving the lateral region of the occipital cortex, temporal cortex, left ventrolateral prefrontal cortex in conceptual processing of the objects and semantic memory (for recent reviews, see [12, 28, 29]). For instance, our last study [3], using fMRI, demonstrated that the selected regions of interest which involve in encoding of the information about a special object category were frontal, temporal, occipital and fusiform areas. The results suggest that the low-frequency phase and high-frequency power of the EEG oscillatory signal reflect stimulus-selective activation patterns arose from the neural responses of those cortical areas generating the oscillations.

In addition, we found that, during the object categorization task, there is an association between IPC and all decoding pattern from phase of frequency bands in various regions of interest (Tables 3, 4). This confirms that the IPC alone can predict the ability to classify single trials of data in individual electrodes in specific frequency bands.

## 5 Conclusion

Summarizing, in this study we applied multivariate analysis technique for predicting the semantic object category related to brain activity. Our approach allows identification of the data feature (phase and power) that has more information about the semantic category of objects. We demonstrated that in the low frequency oscillations the information about the phase of EEG signals is more than the amplitude of electroencephalogram signals to decode the category of objects from the single-trial EEG signals, specifically the low-frequency band (1–4 Hz) information. In contrast, the information of the semantic categories is encoded in the power of high-frequency band (20–30 Hz)

of EEG signals. Moreover, our approach indicated that how the information of objects represented on the EEG signals across the time. However, our results demonstrated that the decoding performance across the time is significantly correlated to the inter-trial phase coherence measure.

We discussed how this study might help studies to find out the machines of object categorization as a high-level cognitive state in human. For future work, we will focus on developing a computational method to increase the classification accuracy. We also are interesting to investigate the relation of different modalities of stimulus, as a picture, as a spoken word, as a written word and their correlation with human conceptual processing.

## References

1. Bedrosian E (1962) A product theorem for hilbert transforms [WWW Document]. [http://www.rand.org/pubs/research\\_memo-randa/RM3439.html](http://www.rand.org/pubs/research_memo-randa/RM3439.html). Accessed on 13 May 2013
2. Behroozi M, Daliri MR (2014) RDL PFC area of the brain encodes sentence polarity: a study using fMRI. *Brain Imaging Behav*. doi:10.1007/s11682-014-9294-z
3. Behroozi M, Daliri MR (2014) Predicting brain states associated with object categories from fMRI data. *J Integr Neurosci* 13:645–667. doi:10.1142/S0219635214500241
4. Behroozi M, Daliri MR, Boyaci H (2011) Statistical analysis methods for the fMRI data. *BCN* 2(4):67–74
5. Carlson TA, Schrater P, He S (2003) Patterns of activity in the categorical representations of objects. *J Cogn Neurosci* 15:704–717. doi:10.1162/jocn.2003.15.5.704
6. Cox DD, Savoy RL (2003) Functional magnetic resonance imaging (fMRI) “brain reading”: detecting and classifying distributed patterns of fMRI activity in human visual cortex. *NeuroImage* 19:261–270
7. Daliri MR, Behroozi M (2013) fMRI: clinical and research applications. *OMICS J Radiol*. doi:10.4172/2167-7964.1000e112
8. Daliri MR, Behroozi M (2014) Advantages and disadvantages of resting state functional connectivity magnetic resonance imaging for clinical applications. *OMICS J Radiol*. doi:10.4172/2167-7964.1000e123
9. Donner TH, Siegel M (2011) A framework for local cortical oscillation patterns. *Trends Cogn Sci* 15:191–199. doi:10.1016/j.tics.2011.03.007
10. Duda PEH, David G, Stork Richard O (2000) *Pattern Classification*, 2nd edn. Wiley-Interscience, New York
11. Fell J, Dietl T, Grunwald T, Kurthen M, Klaver P, Trautner P, Schaller C, Elger CE, Fernández G (2004) Neural bases of cognitive ERPs: more than phase reset. *J Cogn Neurosci* 16:1595–1604. doi:10.1162/0898929042568514
12. Gerlach C (2007) A review of functional imaging studies on category specificity. *J Cogn Neurosci* 19:296–314. doi:10.1162/jocn.2007.19.2.296
13. Gruber T, Trujillo-Barreto NJ, Giabbiconi C-M, Valdés-Sosa PA, Müller MM (2006) Brain electrical tomography (BET) analysis of induced gamma band responses during a simple object recognition task. *NeuroImage* 29:888–900. doi:10.1016/j.neuroimage.2005.09.004

14. Haxby JV, Gobbini MI, Furey ML, Ishai A, Schouten JL, Pietrini P (2001) Distributed and overlapping representations of faces and objects in ventral temporal cortex. *Science* 293:2425–2430. doi:[10.1126/science.1063736](https://doi.org/10.1126/science.1063736)
15. Haynes J-D, Rees G (2006) Decoding mental states from brain activity in humans. *Nat Rev Neurosci* 7:523–534. doi:[10.1038/nrn1931](https://doi.org/10.1038/nrn1931)
16. Hipp JF, Engel AK, Siegel M (2011) Oscillatory synchronization in large-scale cortical networks predicts perception. *Neuron* 69:387–396. doi:[10.1016/j.neuron.2010.12.027](https://doi.org/10.1016/j.neuron.2010.12.027)
17. Ishai A, Ungerleider LG, Martin A, Schouten JL, Haxby JV (1999) Distributed representation of objects in the human ventral visual pathway. *Proc Natl Acad Sci USA* 96:9379–9384
18. Johnson JS, Olshausen BA (2003) Timecourse of neural signatures of object recognition. *J Vis* 3:4. doi:[10.1167/3.7.4](https://doi.org/10.1167/3.7.4)
19. Kamitani Y, Tong F (2005) Decoding the visual and subjective contents of the human brain. *Nat Neurosci* 8:679–685. doi:[10.1038/nn1444](https://doi.org/10.1038/nn1444)
20. Kay KN, Naselaris T, Prenger RJ, Gallant JL (2008) Identifying natural images from human brain activity. *Nature* 452:352–355. doi:[10.1038/nature06713](https://doi.org/10.1038/nature06713)
21. Kayser C, Montemurro MA, Logothetis NK, Panzeri S (2009) Spike-phase coding boosts and stabilizes information carried by spatial and temporal spike patterns. *Neuron* 61:597–608. doi:[10.1016/j.neuron.2009.01.008](https://doi.org/10.1016/j.neuron.2009.01.008)
22. Kohav R (1995) A study of cross-validation and bootstrap for accuracy estimation and model selection. In: Proceedings of the fourth international joint conference on artificial intelligence (San Mateo, CA: Morgan Kaufmann) 2(2):1137–1143
23. Kreiman G (2004) Neural coding: computational and biophysical perspectives. *Phys Life Rev* 1:71–102. doi:[10.1016/j.plev.2004.06.001](https://doi.org/10.1016/j.plev.2004.06.001)
24. Lakatos P, Musacchia G, O’Connell MN, Falchier AY, Javitt DC, Schroeder CE (2013) The spectrotemporal filter mechanism of auditory selective attention. *Neuron* 77:750–761. doi:[10.1016/j.neuron.2012.11.034](https://doi.org/10.1016/j.neuron.2012.11.034)
25. Lopour BA, Tavassoli A, Fried I, Ringach DL (2013) Coding of information in the phase of local field potentials within human medial temporal lobe. *Neuron* 79:594–606. doi:[10.1016/j.neuron.2013.06.001](https://doi.org/10.1016/j.neuron.2013.06.001)
26. Lopour BA, Tavassoli A, Fried I, Ringach DL (2013) Coding of information in the phase of local field potentials within human medial temporal lobe. *Neuron*. doi:[10.1016/j.neuron.2013.06.001](https://doi.org/10.1016/j.neuron.2013.06.001)
27. Makeig S, Westerfield M, Jung T-P, Enghoff S, Townsend J, Courchesne E, Sejnowski TJ (2002) Dynamic brain sources of visual evoked responses. *Science* 295:690–694. doi:[10.1126/science.1066168](https://doi.org/10.1126/science.1066168)
28. Martin A (2007) The representation of object concepts in the brain. *Annu Rev Psychol* 58:25–45. doi:[10.1146/annurev.psych.57.102904.190143](https://doi.org/10.1146/annurev.psych.57.102904.190143)
29. Martin A, Chao LL (2001) Semantic memory and the brain: structure and processes. *Curr Opin Neurobiol* 11:194–201
30. Mathewson KE, Gratton G, Fabiani M, Beck DM, Ro T (2009) To see or not to see: prestimulus alpha phase predicts visual awareness. *J Neurosci Off J Soc Neurosci* 29:2725–2732. doi:[10.1523/JNEUROSCI.3963-08.2009](https://doi.org/10.1523/JNEUROSCI.3963-08.2009)
31. Mitchell TM, Shinkareva SV, Carlson A, Chang K-M, Malave VL, Mason RA, Just MA (2008) Predicting human brain activity associated with the meanings of nouns. *Science* 320:1191–1195. doi:[10.1126/science.1152876](https://doi.org/10.1126/science.1152876)
32. Montemurro MA, Rasch MJ, Murayama Y, Logothetis NK, Panzeri S (2008) Phase-of-firing coding of natural visual stimuli in primary visual cortex. *Curr Biol CB* 18:375–380. doi:[10.1016/j.cub.2008.02.023](https://doi.org/10.1016/j.cub.2008.02.023)
33. Mormann F, Lehnertz K, David PE, Elger C (2000) Mean phase coherence as a measure for phase synchronization and its application to the EEG of epilepsy patients. *Phys Nonlinear Phenom* 144:358–369. doi:[10.1016/S0167-2789\(00\)00087-7](https://doi.org/10.1016/S0167-2789(00)00087-7)
34. Ng BSW, Logothetis NK, Kayser C (2013) EEG phase patterns reflect the selectivity of neural firing. *Cereb Cortex* 1991(23):389–398. doi:[10.1093/cercor/bhs031](https://doi.org/10.1093/cercor/bhs031)
35. Ng BSW, Logothetis NK, Kayser C (2013) EEG phase patterns reflect the selectivity of neural firing. *Cereb Cortex* 1991(23):389–398. doi:[10.1093/cercor/bhs031](https://doi.org/10.1093/cercor/bhs031)
36. Rousselet GA, Husk JS, Bennett PJ, Sekuler AB (2007) Single-trial EEG dynamics of object and face visual processing. *NeuroImage* 36:843–862. doi:[10.1016/j.neuroimage.2007.02.052](https://doi.org/10.1016/j.neuroimage.2007.02.052)
37. Russell S, Norvig P (2009) Artificial intelligence: a modern approach, 3rd edn. Prentice Hall, Upper Saddle River
38. Sauseng P, Klimesch W (2008) What does phase information of oscillatory brain activity tell us about cognitive processes? *Neurosci Biobehav Rev* 32:1001–1013. doi:[10.1016/j.neubiorev.2008.03.014](https://doi.org/10.1016/j.neubiorev.2008.03.014)
39. Schyns PG, Thut G, Gross J (2011) Cracking the code of oscillatory activity. *PLoS Biol* 9:e1001064. doi:[10.1371/journal.pbio.1001064](https://doi.org/10.1371/journal.pbio.1001064)
40. Shah AS, Bressler SL, Knuth KH, Ding M, Mehta AD, Ulbert I, Schroeder CE (2004) Neural dynamics and the fundamental mechanisms of event-related brain potentials. *Cereb Cortex* 14:476–483. doi:[10.1093/cercor/bhh009](https://doi.org/10.1093/cercor/bhh009)
41. Siegel M, Warden MR, Miller EK (2009) Phase-dependent neuronal coding of objects in short-term memory. *Proc Natl Acad Sci*. doi:[10.1073/pnas.0908193106](https://doi.org/10.1073/pnas.0908193106)
42. Supp GG, Schlögl A, Trujillo-Barreto N, Müller MM, Gruber T (2007) Directed cortical information flow during human object recognition: analyzing induced eeg gamma-band responses in brain’s source space. *PLoS ONE* 2:e684. doi:[10.1371/journal.pone.0000684](https://doi.org/10.1371/journal.pone.0000684)
43. Taghizadeh-Sarabi M, Daliri MR, Niksirat KS (2014) Decoding objects of basic categories from electroencephalographic signals using wavelet transform and support vector machines. *Brain Topogr*. doi:[10.1007/s10548-014-0371-9](https://doi.org/10.1007/s10548-014-0371-9)
44. VanRullen R, Busch NA, Drewes J, Dubois J (2011) Ongoing EEG phase as a trial-by-trial predictor of perceptual and attentional variability. *Front Percept Sci* 2:60. doi:[10.3389/fpsyg.2011.00060](https://doi.org/10.3389/fpsyg.2011.00060)
45. Varela F, Lachaux J-P, Rodriguez E, Martinerie J (2001) The brainweb: phase synchronization and large-scale integration. *Nat Rev Neurosci* 2:229–239. doi:[10.1038/35067550](https://doi.org/10.1038/35067550)



**Mehdi Behroozi** received the M.Sc. degree in Biomedical engineering in 2012. He is currently working toward the Ph.D. degree in Neuroscience at the Department of Biopsychology, RUHR University Bochum, Bochum, Germany.



**Mohammad Reza Daliri** is an Associate Professor in Iran University of Science and Technology (IUST), Tehran, Iran. His main research interests include brain signal and image processing, computational and cognitive neuroscience.



**Babak Shekarchi** is an Associate Professor of radiology in AJA University of Medical Science, Tehran, Iran. His main research interests include diagnostic imaging and interventional radiology.